NATIONAL ADVISORY COMMITTEE FOR AERONAUTICS

TECHNICAL NOTE 3652

EXPERIMENTAL INVESTIGATION OF AIR-FLOW UNIFORMITY AND PRESSURE LEVEL ON WIRE CLOTH FOR TRANSPIRATION-COOLING APPLICATIONS

By Patrick L. Donoughe and Roy A. McKinnon

Lewis Flight Propulsion Laboratory
Cleveland, Ohio

Washington

January 1956

NATIONAL ADVISORY COMMITTEE FOR AERONAUTICS

TECHNICAL NOTE 3652

EXPERIMENTAL INVESTIGATION OF AIR-FLOW UNIFORMITY AND PRESSURE LEVEL ON WIRE CLOTH FOR TRANSPIRATION-COOLING APPLICATIONS

By Patrick L. Donoughe and Roy A. McKinnon

SUMMARY

The problem of producing uniform air flow through a calendered or cold-rolled sheet of brazed stainless-steel corduroy wire cloth was investigated on 20X250 mesh cloth in regions of low permeability. The effect of exit pressure level was determined at various exit pressures on 20X200, 20X250, and 28X500 mesh wire cloth. In addition, permeability and strength data were obtained for 20X200 mesh wire cloth to supplement results previously published on other meshes.

It was found that for permeability coefficients of the order of 10^{-9} inch^2 control of the calendering process to ±0.0002 inch should yield air flow uniform within ±5 percent. Results showed that available methods may be used to predict, within experimental accuracy, the effect of exit pressure level. The values of permeability and strength of the 20X200 mesh wire cloth were close to those already available for the other meshes. The reduced tensile strength of 20X200 and 20X250 mesh wire cloth, in the direction of the primary stresses, was $1\frac{1}{2}$ to 3 times as great as the strength of the best porous sintered materials presently available.

INTRODUCTION

The superior cooling effectiveness attainable by the transpiration cooling of a structure in a high-temperature, high-velocity gas stream is discussed in reference 1. In this method of cooling, the part to be cooled is made of a porous material having a predetermined permeability; the coolant is forced through the porous wall, cooling the wall as it passes through and forming a protective insulating layer on the surface exposed to the hot gas stream. One material, investigated in reference 2, that could possibly be used for transpiration-cooled walls is stainless-steel corduroy wire cloth.

---

[1]Supersedes recently declassified NACA RM E52E16 by Patrick L. Donoughe and Roy A. McKinnon, 1952.

be controlled by calendering or cold rolling. Permeability and strength characteristics were also obtained for three different meshes, 20X250, 20X350, and 28X500. Comparison with available results on porous sintered materials revealed that these stainless-steel wire cloths offer a much wider range of permeability and possess ultimate tensile strengths, in the direction of primary stresses (coinciding with the direction of the larger number of wires), two to three times the ultimate tensile strength of the porous sintered materials.

In the application of transpiration cooling to turbine blades, the blade contours will probably be formed from a sheet of brazed stainless-steel wire cloth which has been calendered to obtain desired permeabilities. For porous turbine blades, the required permeability coefficient is expected to be of the order of 10^{-9} inch^2. In this range of low permeability, small changes in thickness reduction by calendering produced large changes in permeability (reference 2). Consequently, the problem of producing a sheet of cloth with a uniform desired permeability requires further study because of the close tolerances necessary in calendering.

At altitude, the pressure level and distribution around turbine blades are much different from those at sea-level conditions. Calculations also indicate that the maintenance of the required coolant flow at altitude requires special study. Permeability measurements on porous materials are usually obtained at ambient exit conditions and extrapolated to other conditions by the use of some theoretical relation such as Darcy's law. Air-flow measurements on the wire cloth made at different exit pressures and pressure levels give a check as to the validity of such extrapolations.

The pressure drop for a given flow is shown in reference 2 to be roughly proportional to the thickness of the wire cloth. For a given pressure drop, a cloth with large wires requires less thickness reduction than one with small wires and because of the lesser reduction uniform permeability is more easily obtained. In addition, a structure formed with a thicker cloth should be stiffer and require less reinforcement. A commercially available 20X200 mesh wire cloth is thicker than the cloth investigated in reference 2; information about this mesh, similar to that presented for the other meshes, is desirable.

An experimental investigation was carried out at the NACA Lewis laboratory in order to obtain information on the points previously specified. Results are presented herein regarding (1) uniformity of air flow in the region of low permeability coefficient (10^{-9} in.^{2}) for 20X250 mesh, (2) effect of pressure levels for pressure-square differences up to 1450 pounds^2 per inch^4 on air flow through 20X200, 20X250, and 28X500 mesh, and (3) permeability and strength data for a 20X200 mesh stainless-steel wire cloth.

APPARATUS AND PROCEDURE

Description and Preparation of Wire Cloth

Various meshes of stainless-steel wire cloth were utilized to obtain uniformity of air-flow and pressure-level effects. The specifications and the preparation of the 20X250 and the 28X500 mesh cloths are discussed in reference 2. The same material, AISI type 304 stainless steel, was used for the 20X200 mesh wire cloth. This mesh has 20 wires per inch (0.011 in. diam) in the crosswise, or warp, direction and 200 wires per inch (0.010 in. diam) in the lengthwise, or shoot, direction. Front and side views of the 20X200 mesh wire cloth, as woven and after calendering, are shown in figures 1(a) and 1(b). The average thickness of this mesh as woven was measured as 0.0307 inch, which is 15 percent greater than the thickest mesh reported in reference 2; this thickness was increased to an average of 0.0312 inch by brazing. In the brazing process, the cloth as woven was sprayed with a silver brazing alloy (1260° F melting point) and dipped into a salt bath at 1400° F until the sprayed alloy was brazed to the surface of the wires (about 30 sec). Views of the cloth after brazing and after calendering are shown in figures 1(c) and 1(d). This preparation was the same as that described in reference 2. The cloth containing no brazing material is herein referred to as "unbrazed wire cloth," and the sprayed and heated cloth as "brazed wire cloth."

Thickness and Air-Flow Measurements

Uniformity of thickness and air flow were checked on the 20X250 mesh wire cloth with disks $1\frac{1}{2}$ inches in diameter stamped from sheets which had been calendered to a nominal thickness. The $1\frac{1}{2}$-inch diameter was used only to facilitate stamping of the disks. The diameter of that portion of the disk exposed to air flow in the test section was 1.31 inches. The thicknesses of the disks were measured with micrometers. Five thickness measurements were made on each disk, one in the center and the others 1/4 inch from the disk edge spaced at 90°. Prior to stamping, orientation marks were made so that the thickness measurements for each disk would be in the same relative position with respect to the calendered sheet.

The method of sealing the test specimens, shown in figure 2, was different from that described in reference 2. In place of metal gaskets, paper gaskets (0.004 in. thick) were placed above and below the rim of the disk which lies in a groove of a pipe flange. A rubber O-ring, 2 inches in diameter, was located in another groove outside the disk. When a mating pipe flange was drawn tightly, the paper gaskets

and the rubber O-ring were compressed and formed an effective seal. Only one disk, or one layer of wire cloth, was used in the current experiments because it was found in reference 2 that the number of layers used as the test specimen produces a negligible effect on the permeability coefficient.

The equipment used to obtain air-flow data for the 20X200 mesh cloth was similar to that described in reference 2 but some modifications were necessary for the pressure-level investigations. The apparatus is schematically shown in figure 2. Air at room temperature and a pressure of 120 pounds per inch^2 gage was filtered, passed through a pressure regulator, controlled by a hand valve, and measured by a rotameter prior to entering the wire cloth. (It was noted that with a standard commercial-type filter, no noticeable clogging of the wire cloth occurred.)

In the pressure-level experiments on the 20X200, 20X250, and 28X500 mesh cloths, it was necessary to control the exit pressure, or the pressure of the air leaving the specimen. To this end, hand valves were placed in the exit line which was connected to the altitude exhaust system to provide exit pressures below atmospheric. Exit pressures above atmospheric were obtained by using the hand valves as throttles and exhausting the air into the room. During the tests, pressures on both sides of the specimens and weight flow through them were measured. Exit pressures of 36.8, 29.4, 11.76, and 8.82 pounds per inch^2 absolute were maintained during the pressure-level experiments. In the flow uniformity and 20X200 mesh studies, the exit pressure was atmospheric.

Strength Measurements

Room-temperature strength measurements of the 20X250, 20X350, and 28X500 mesh cloths are described in reference 2. The strength of the 20X200 mesh cloth was determined in a similar manner. The specimens, 0.6 inch wide and 12 inches long, were tinned at the ends to obtain better gripping in the jaws of the testing machine. A constant rate of loading was used rather than the 100-pound increments used in reference 2.

METHODS OF CORRELATION AND CALCULATION

Reduction of Air-Flow Data to Standard Conditions

The examination of the air-flow data for pressure-level effects, uniformity, and permeability was based on the following relation, given in reference 3, for the flow of a gas through the plane wall of a porous material:

$$\frac{p_1^2-p_2^2}{\tau} = \alpha\,(2RT\mu)\,G + \beta\left(\frac{2RT}{g}\right)G^2 \tag{1}$$

where α is termed the viscous resistance coefficient and β the inertial resistance coefficient. (Symbols are defined in appendix.) It is noted in reference 4 that equation (1) when solved for G may be written

$$G/\mu = \sqrt{C_1^2 + C_2\frac{p_1^2-p_2^2}{\mu^2 T\tau}} - C_1 \tag{2}$$

with $C_1 = \alpha g/2\beta$, and $C_2 = g/2\beta R$ being constant for each specimen so that

$$G/\mu = f_1\left(\frac{p_1^2-p_2^2}{\mu^2 T\tau}\right) \tag{3}$$

Equation (3) can be used to reduce the data to standard conditions by introduction of μ_o and $\mu_o^2 T_o$, where the subscript o signifies NACA standard temperature of 518° R. Thus, equation (3) becomes

$$G\,\frac{\mu_o}{\mu} = f_2\left(\frac{p_1^2-p_2^2}{\tau}\,\frac{\mu_o^2 T_o}{\mu^2 T}\right) \tag{4}$$

Equation (4) is utilized as the correlation equation for the air-flow data in this report by plotting $\frac{p_1^2-p_2^2}{\tau}\,\frac{\mu_o^2 T_o}{\mu^2 T}$ against $G\,\frac{\mu_o}{\mu}$ for a porous specimen. The logarithm of $\frac{p_1^2-p_2^2}{\tau}\,\frac{\mu_o^2 T_o}{\mu^2 T}$ is herein referred to as the "pressure-drop parameter" for discussion purposes. The viscosity μ and the temperature correction factors $\frac{\mu_o}{\mu}$ and $\left(\frac{\mu_o}{\mu}\right)^2\frac{T_o}{T}$ are given in table I as functions of temperature.

Calculation of Permeability, Porosity, and Strength

Comparison of results from tests on different porous materials is usually made on the basis of permeability. A permeability coefficient K based on Darcy's law is given by

$$\frac{p_1^2-p_2^2}{\tau} = \frac{1}{K}(2RT\mu)\,G \tag{5}$$

A linear relation between the pressure-square difference per unit thickness and the mass rate of flow is assumed in this law. Actually the relation is not quite linear; the use of equation (1) is therefore recommended in reference 3. In reference 2 equations (1) and (5) were equated and solved for K with the result that

$$K = \frac{1}{\alpha}\frac{1}{1+\frac{\beta}{\alpha\mu g}G} \tag{6}$$

The permeability values given in this report and in reference 2 were obtained in the following way: The method of least squares (reference 5) was applied to equation (1) and α and β were calculated for a series of mass flows and pressure-square differences for a given reduction in the original thickness of the wire cloth. In order to make a comparison with results obtained in previous investigations, equation (6) with $G = 0$ was used and K is therefore the reciprocal of α. Both α and β were calculated because the air-flow data for the wire cloth fit equation (1) and not equation (5). Such an evaluation method eliminates the variation in permeability coefficient with pressure level reported in reference 6 for a given specimen. Values of β/α were of the order of 7×10^{-4} inch for the 20×200 mesh wire cloth.

The porosity of a porous specimen is defined as the ratio of the volume of voids to the total volume. The equation used for obtaining the porosity of brazed stainless-steel corduroy wire cloth, derived in reference 2, is

$$f = 1 - \frac{1}{\tau}\left(\frac{1}{\gamma_s}\frac{W_s}{A} + \frac{1}{\gamma_b}\frac{W_b}{A}\right) \tag{7}$$

The porosities of the wire cloths with different reductions in original thickness were calculated by use of equation (7). The weight per unit surface area of the unbrazed material is W_s/A and the difference in weight per unit surface area between the brazed and unbrazed material is W_b/A. (For the 18-8 stainless steel, γ_s was taken as 0.285 lb/in.^{3} and for the brazing alloy, γ_b was taken as 0.344 lb/in.^{3}.)

The ultimate tensile strength of a material is defined as the force required to break or rupture the specimen divided by the cross-sectional area of the specimen,

$$\sigma = F/a \tag{8}$$

In reference 2, it is pointed out that for aircraft structural elements where weight is an important factor, a better strength criterion is a reduced tensile strength given by

$$\sigma' = \frac{F}{W/L}\gamma_s = \frac{\sigma\gamma_s}{\gamma} \tag{9}$$

Both the ultimate tensile strength and the reduced tensile strength were calculated for the 20X200 mesh wire cloth by use of equations (8) and (9) with the substitution of the measured values of breaking force, area, weight, and length for the different reductions in original thickness.

It is shown in reference 2 that for porous sintered materials the relation between the reduced tensile strength and ultimate tensile strength is

$$\sigma' = \frac{\sigma}{1-f} \tag{10}$$

Where strengths of these materials are given herein, this relation, which credits the porous material with its lighter weight, is used.

RESULTS AND DISCUSSION

Air-Flow Uniformity for Calendered Wire Cloth

The air-flow uniformity tests were made on two sheets of 20X250 mesh stainless-steel wire cloth calendered to nominal reductions of 36 percent and 40 percent of the original thickness, respectively. Because any nonuniformity in thickness will probably result in a nonuniform air flow, detailed thickness measurements were made as noted in the "APPARATUS AND PROCEDURE" section. The measured thicknesses of the 20X250 mesh wire-cloth disks are shown in figures 3(a) and 3(b) for specimens reduced in the calendering process 36 and 40 percent, respectively. Sketches that show the disk location on the sheet are included in these figures. The average thicknesses of the disks from the right sides of the sheets were less than those of the other disks. The thinner disks were expected to pass less air flow for a given pressure drop because of the decreased permeability.

Air-flow data are presented in figure 4(a) for the sheet of 20X250 mesh wire cloth that was reduced 36 percent in thickness by calendering; the pressure-drop parameter is plotted against the corrected mass flow through the disks. Rather than show the data for all 15 disks on one ordinate scale, five plots are presented; each plot is for three disks at the same y position. A curve representing the average of all the data points is drawn through each set of data. The 36-percent reduction in the original thickness of this piece of wire cloth corresponds to a permeability coefficient of about $6X10^{-9}$ inch^2 (range for turbine blades); the air flow may be considered uniform within ±5 percent. For lesser thickness reductions, the air flow should be more uniform because of the permeability-thickness reduction characteristics of the wire cloth.

The air-flow data for the sheet reduced 40 percent in thickness are shown in figure 4(b); again, the same curve is drawn for both plots. Disks 1 and 4, which showed greater thickness reductions (fig. 3(b)), passed about 30 percent less mass flow for a given value of the pressure-drop parameter. The 40-percent reduction, which corresponds to a permeability coefficient of about 10^{-10} inch^2, requires closer control of the final thickness of the wire cloth than is required for the 36-percent reduction for the same uniformity in air flow. Such control may be possible by improved calendering techniques.

Effect of Exit Pressure or Pressure Level on Air Flow

Three different meshes, having various thickness reductions, were used to determine any effects on air flow due to different exit pressures or pressure levels. The results in the form of the pressure-drop parameter against mass flow are shown in figure 5(a) for the 20X200 mesh, in figure 5(b) for the 20X250 mesh, and in figure 5(c) for the 28X500 mesh. Although the exit pressures ranged from 0.6 to 2.5 atmospheres and the pressure-square differences ranged up to 1450 pounds^2 per inch^4, the resulting variations in air flow were small and are represented with good accuracy by equations (1) and (6) in the range in which

$$0 \leq G \frac{\mu_o}{\mu} \leq 0.004.$$

Permeability and Strength of 20X200 Mesh Wire Cloth

The results of the permeability tests on the 20X200 mesh wire cloth are plotted as the pressure-drop parameter against the corrected mass flow in figure 6(a) for the unbrazed wire cloth and in figure 6(b) for the brazed wire cloth. Each of the figures contains the results of various reductions in thickness by calendering. The effect of brazing

the cloth is evidently more apparent for the larger reductions in thickness. This effect is shown by a comparison of the specimens reduced 42 and 23 percent (figs. 6(a) and 6(b)). At a given value of the pressure-drop parameter, the brazed specimen that was reduced about 42 percent in thickness passed only about 1/5 as much mass flow as did the unbrazed specimen. The mass flow through the specimens that were reduced about 23 percent in thickness was nearly the same whether brazed or unbrazed.

This same effect is also illustrated in figure 7 where the calculated permeability coefficients are given as a function of the reduction of thickness produced by calendering. Also included are curves showing results from reference 2 for the three meshes investigated therein. The reason for the discrepancy between the previous results and those obtained with the 20X200 mesh wire cloth is not readily apparent. The scatter of the data in reference 2 made the curves difficult to establish; and the lack of data scatter for the results on the 20X200 mesh is perhaps attributable to refinements in sealing made in the test apparatus.

The porosities of the 20X200 mesh cloth were calculated by use of equation (7). Because both porosity and permeability are functions of the reduction in thickness, it is possible to show the porosity as a function of the permeability coefficient. This relation is shown in figure 8 where porosity is plotted against permeability coefficient for the 20X200 mesh wire cloth, brazed and unbrazed. Also included are results from reference 2 for different meshes and some values for the porous sintered materials recently reported in references 6 and 7. The 20X200 mesh wire cloth shows the same trends as the meshes previously investigated and the permeability range is much greater than that of the porous sintered materials (fig. 8).

In figures 9(a) and 9(b), the ultimate tensile strengths and reduced tensile strengths, obtained by use of equations (8) and (9), are given as functions of the reduction in thickness of the unbrazed and brazed wire cloth. Also included as a dashed line are some results from reference 2 for the 20X250 mesh cloth. Strength data obtained in the present investigation for the brazed 20X250 mesh are also shown in figure 9(b). The reduced strengths of the 20X200 mesh cloth are not very different from those of the 20X250 mesh.

Finally, the reduced tensile strength of the 20X200 mesh wire cloth was plotted against the permeability coefficient in figure 10 along with results from reference 2 for other meshes and from references 6 and 7 for porous sintered materials. Average strength results from reference 7, calculated by use of equation (10) are represented by curve 8. The strength range of the 20X200 mesh wire cloth is similar to that obtained for the 20X250 mesh. Much higher strengths than previously reported are shown for the porous sintered materials because of the additional process of coining and resintering. The reduced

tensile strengths of the 20X200 and 20X250 mesh wire cloth, in the direction of the primary stresses, however, are still $1\frac{1}{2}$ to 3 times the strengths of the porous sintered materials.

SUMMARY OF RESULTS

An experimental investigation was conducted with stainless-steel corduroy wire cloth to determine: uniformity of air flow in the region of low permeability coefficient (10^{-9} in.^{2}) for brazed and calendered 20X250 mesh; effect of pressure level on air flow for brazed and calendered 20X200, 20X250, and 28X500 meshes; and permeability and strength data for brazed and unbrazed 20X200 mesh with different amounts of calendering. The following results were obtained:

1. For a reduction of 36 percent in the original thickness of the wire cloth, control of the calendering to ±0.0002 inch yielded uniform air flow within ±5 percent. Reduction of 40 percent would require closer control of calendering for the same air flow uniformity.

2. The effect of pressure level for exit pressures from 0.6 to 2.5 atmospheres was predicted by known analytical relations, within experimental accuracy, in the corrected mass flow range up to 0.004 pound per second-inch^2.

3. The permeability and the porosity data for the 20X200 mesh wire cloth were in the same range as the data for other meshes previously investigated, but for a given pressure-square difference less thickness reduction was necessary for the 20X200 mesh wire cloth.

4. The reduced tensile strengths of the 20X200 mesh wire cloth were about the same as those of the 20X250 mesh. The reduced tensile strength of the cloth, in the direction of the primary stresses, was $1\frac{1}{2}$ to 3 times as large as the strength of the best porous sintered materials presently available.

Lewis Flight Propulsion Laboratory
National Advisory Committee for Aeronautics
Cleveland, Ohio, May 16, 1952

APPENDIX - SYMBOLS

The following symbols are used in this report:

A	surface area, $in.^2$
a	cross-sectional area, $in.^2$
C_1	$\frac{\alpha g}{2\beta}$, sec^{-2}
C_2	$\frac{g}{2\beta R}$, $(in.)(^oR)/sec^2$
F	rupture force, lb
f	porosity, dimensionless
f_1, f_2	functions
G	mass rate of air flow, $lb/(sec)(in.^2)$
g	gravitational constant, $in./sec^2$
K	permeability coefficient, $in.^2$
L	length, in.
p	static pressure of air, $lb/in.^2$
R	gas constant for air, $in./^oR$
T	static temperature of air, ^oR
W	weight, lb
x	direction perpendicular to calendering, or direction of crosswise wires
y	direction parallel to calendering, or direction of lengthwise wires
α	viscous resistance coefficient, $in.^{-2}$
β	inertial resistance coefficient, $in.^{-1}$
γ	weight per unit volume of specimen, $lb/in.^3$

μ absolute viscosity of air, (lb)(sec)/in.^{2}

σ tensile strength, lb/in.^{2}

σ' reduced tensile strength, lb/in.^{2}

τ thickness of porous material, in.

Subscripts:

1 side of porous material at high pressure

2 side of porous material at low pressure

b brazed

o NACA standard temperature of 518° R

s steel

REFERENCES

1. Eckert, E. R. G., and Esgar, Jack B.: Survey of Advantages and Problems Associated with Transpiration Cooling and Film Cooling of Gas Turbine Blades. NACA RM E50K15, 1951.

2. Eckert, E. R. G., Kinsler, M R., and Cochran, R. P.: Wire Cloth as Porous Material for Transpiration-Cooled Walls. NACA RM E51H23, 1951.

3. Green, Leon, Jr.: Fluid Flow Through Porous Metals. Prog. Rep. No. 4-111, JPL, CIT Aug. 19, 1949 (Ordnance Dept. Contract No. W-04-200-ORD-455.)

4. Bartoo, Edward R., Schafer, Louis J., Jr., and Richards, Hadley T.: Experimental Investigation of Coolant-Flow Characteristics of a Sintered Porous Turbine Blade. NACA RM E51K02, 1952.

5. Lipka, Joseph: Graphical and Mechanical Computations. Part II - Experimental Data. John Wiley & Sons, Inc., 1921, p. 124.

6. Reen, O. W., and Lenel, F. V.: Production of Porous Metal Compacts Bi-Monthly Prog. Rep. No. 8, Powder Metallurgy Lab., Rensselaer Polytechnic Inst., August 6, 1951. (Navy Research Contract Noa(s) 11022).

7. Comstock, Gregory J., Mott, Lambert H., Bradbury, John D., and Grinthal, Robert D.: Navy Project for Investigation of Porous Material From Spherical Metal Powders. Bi-Monthly Prog. Rep. No. 6, Powder Metallurgy Laboratory, Stevens Inst. of Tech., September 30, 1951. (BuAer. Contract Noas 51-185-c).

8. Keenan, Joseph H., and Kaye, Joseph: Gas Tables. John Wiley & Sons, Inc., 1948, p. 34.

TABLE I - TEMPERATURE CORRECTION FACTORS

Static temperature of air T ($^{\circ}R$)	Absolute viscosity of air[1] μ (lb-sec/in.2)	Temperature correction factors	
		$\frac{\mu_o}{\mu}$	$\left(\frac{\mu_o}{\mu}\right)^2 \frac{T_o}{T}$
400	21.6×10^{-10}	1.210	1.8960
450	23.5	1.110	1.4183
500	25.5	1.025	1.0893
518	26.1	1.000	1.0000
550	27.2	.960	.8685
600	29.1	.896	.6936
650	30.9	.846	.5706
700	32.6	.801	.4751
750	34.1	.766	.4050
800	35.8	.729	.3440
850	37.3	.699	.2981
900	38.6	.676	.2630
1000	41.4	.630	.2057
1100	44.3	.590	.1640
1200	47.1	.555	.1330
1300	49.6	.526	.1103
1400	52.2	.500	.0925
1500	54.6	.478	.0790
1600	57.0	.458	.0680
1700	59.1	.442	.0594
1800	61.3	.426	.0522
1900	63.2	.413	.0465
2000	65.2	.401	.0416
2100	67.1	.389	.0373
2200	69.1	.378	.0337
2300	71.0	.368	.0305
2400	73.0	.358	.0277

[1]Values obtained from reference 8.

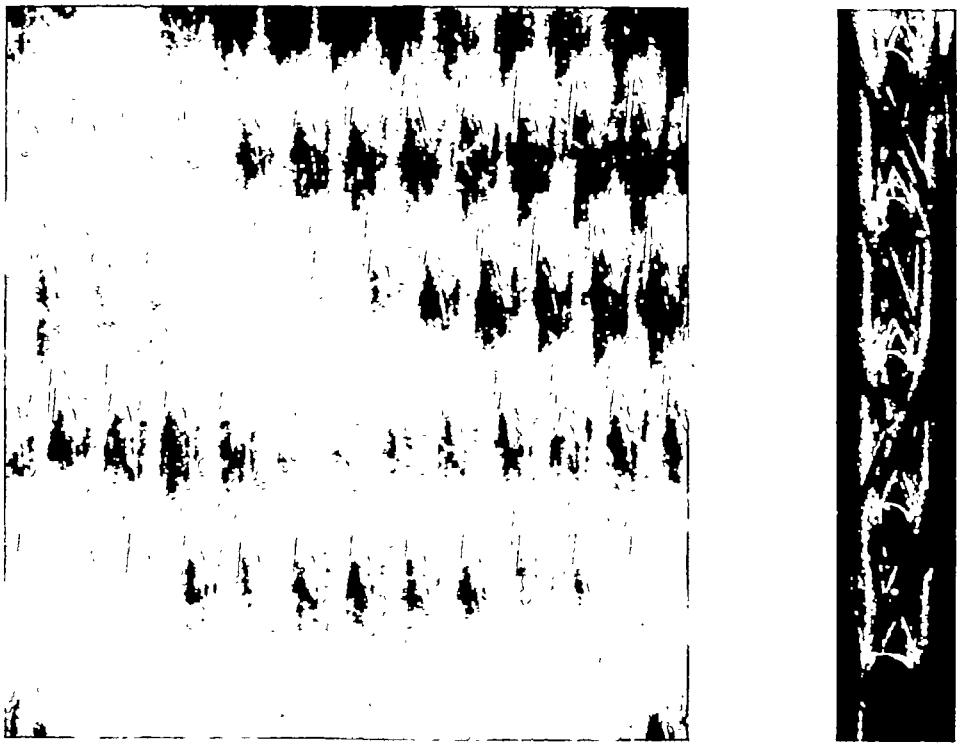

(a) Unbrazed and uncalendered.

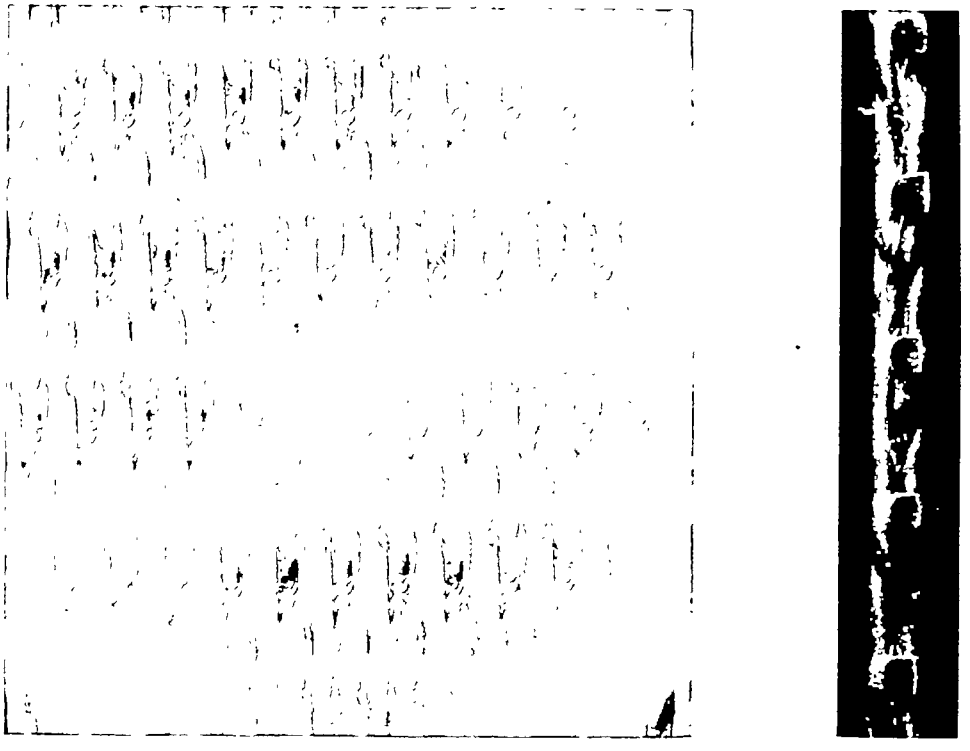

C-29729

(b) Unbrazed and calendered.

Figure 1. - Photographs of 20×200 mesh stainless-steel corduroy wire cloth; X10.

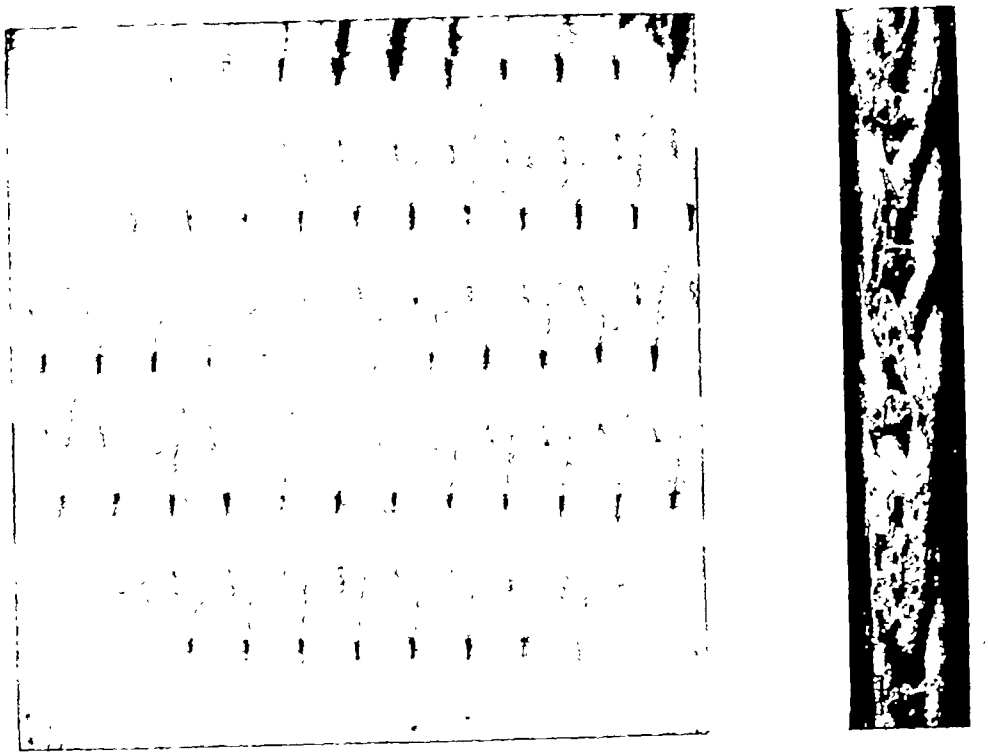

(c) Brazed and uncalendered.

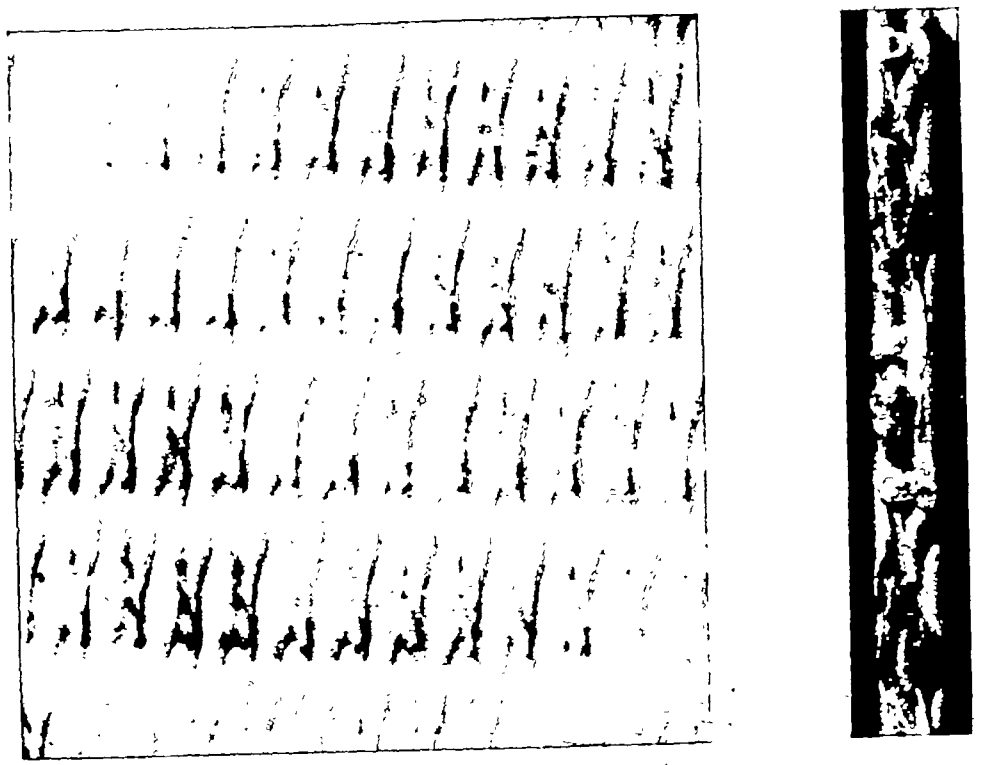

C-29730

(d) Brazed and calendered.

Figure 1. - Concluded. Photographs of 20×200 mesh stainless-steel corduroy wire cloth; X10.

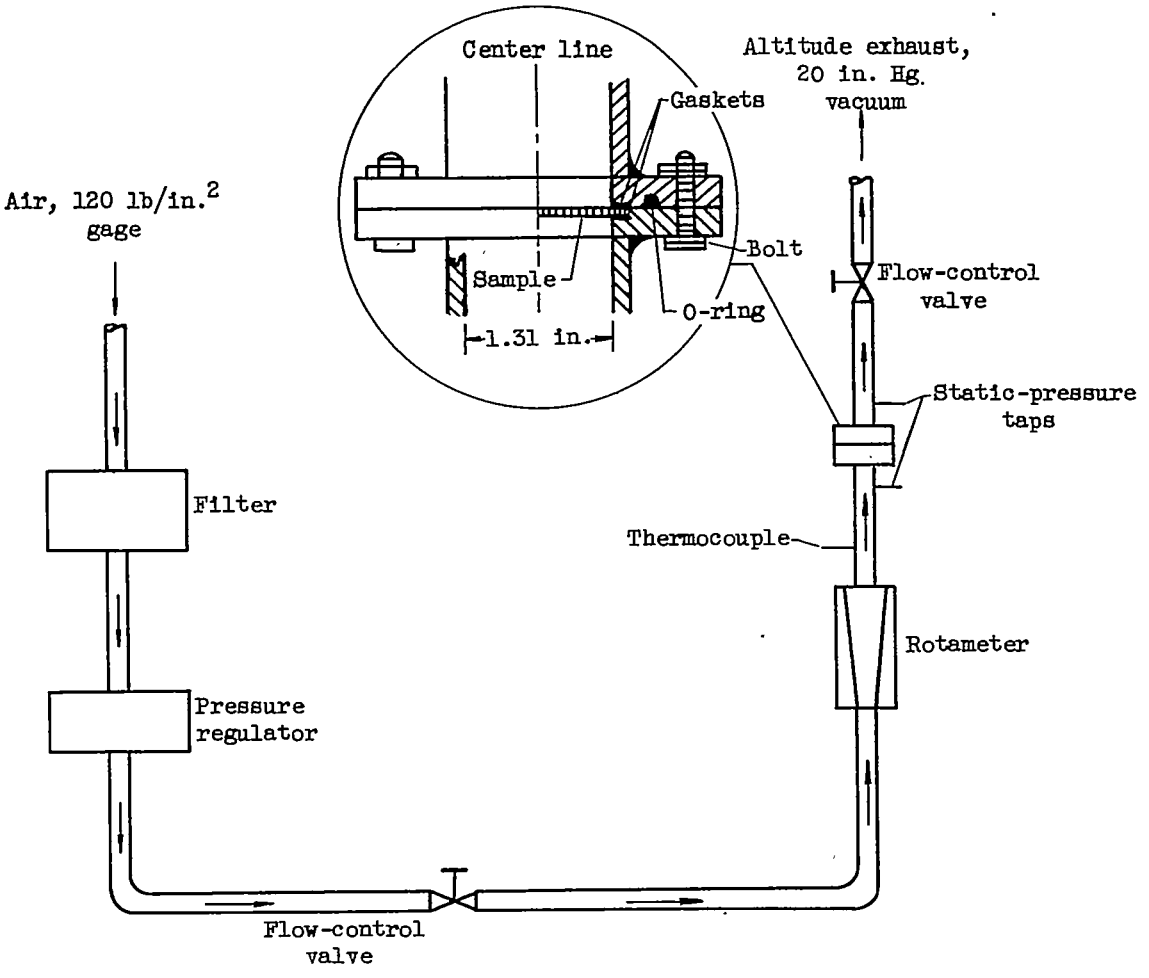

Figure 2. - Schematic diagram of equipment used for measuring air flow through specimens of wire cloth.

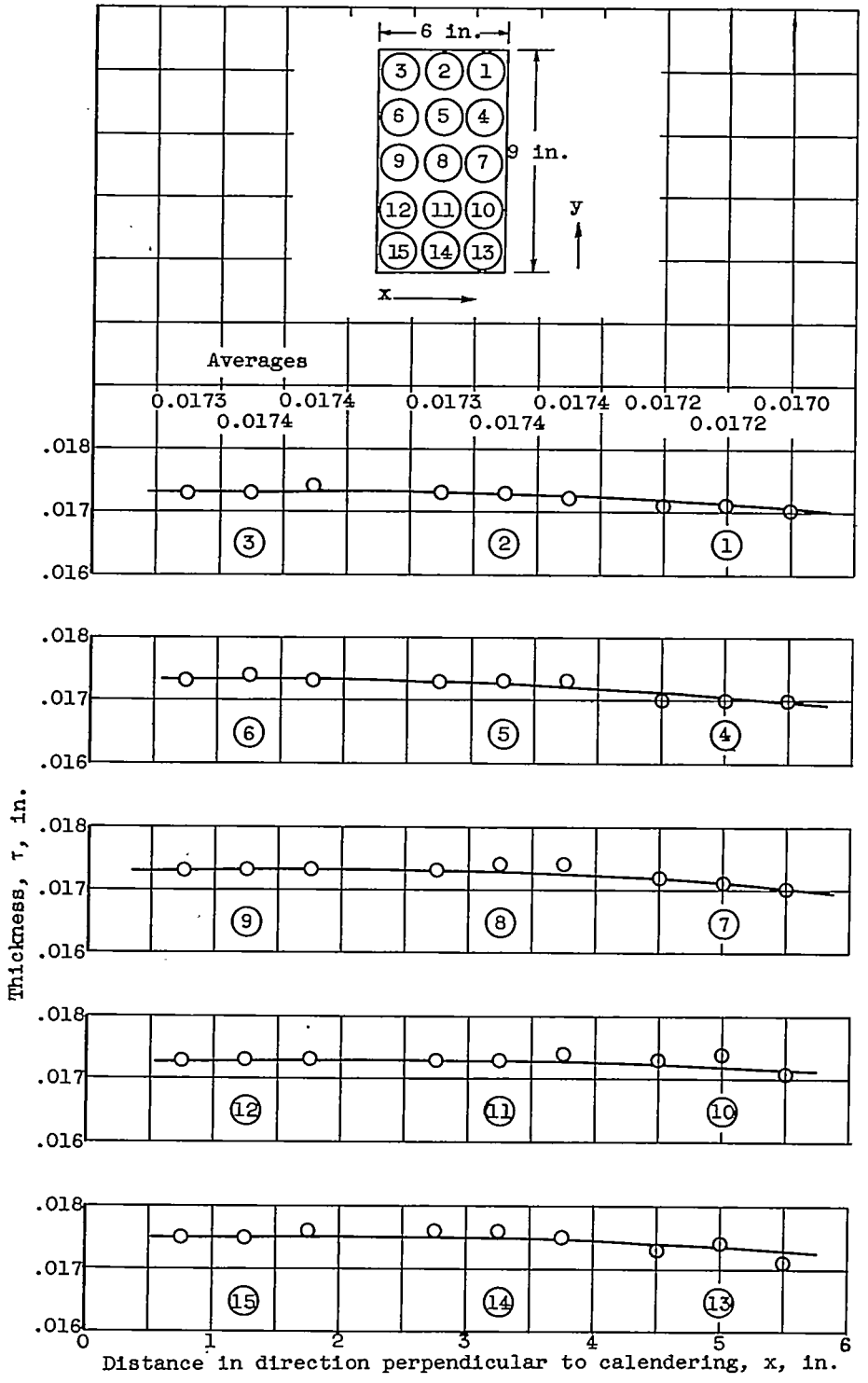

(a) Thickness reduction, 36 percent.

Figure 3. - Thickness measurements of brazed 20x250 mesh wire cloth.

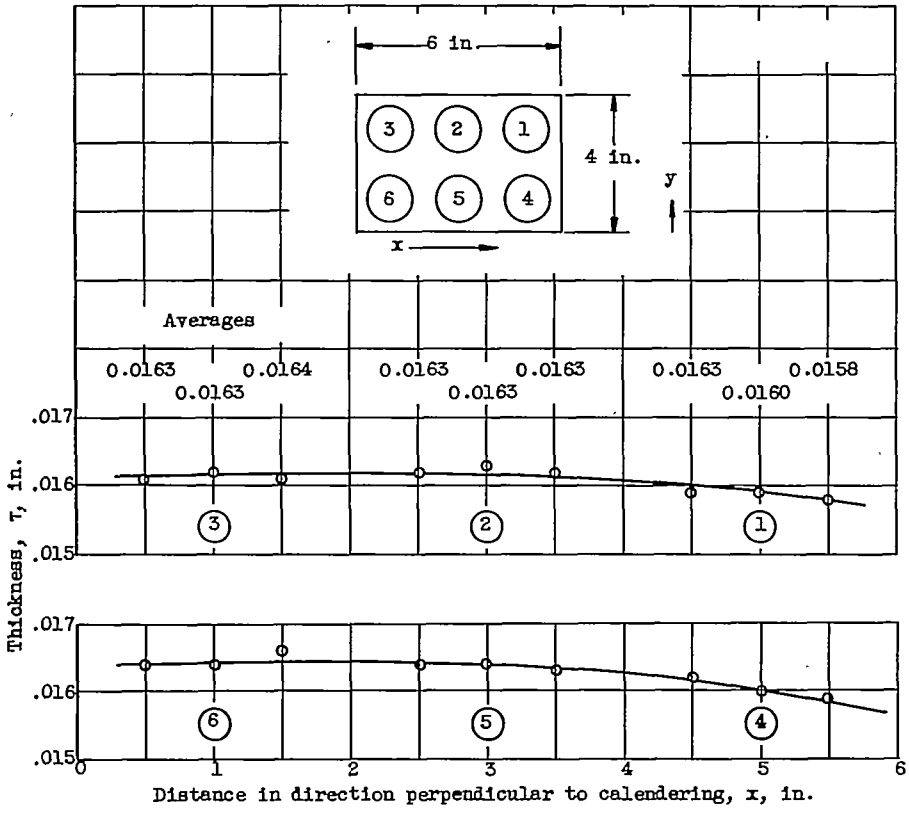

(b) Thickness reduction, 40 percent.

Figure 3. - Concluded. Thickness measurements of brazed 20x250 mesh wire cloth.

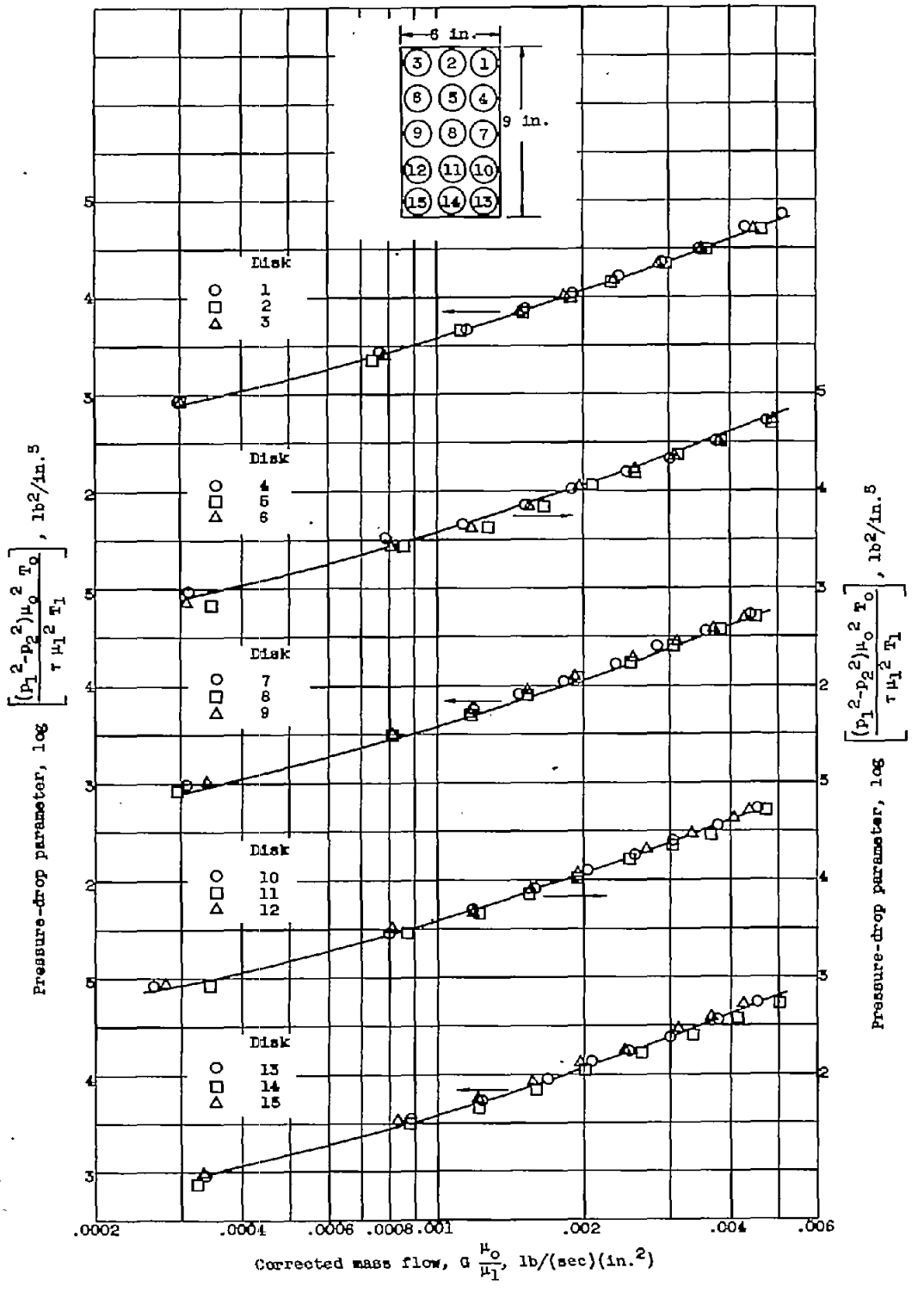

(a) Thickness reduction, 38 percent.

Figure 4. - Uniformity of air flow through brazed 20x250 mesh wire cloth.

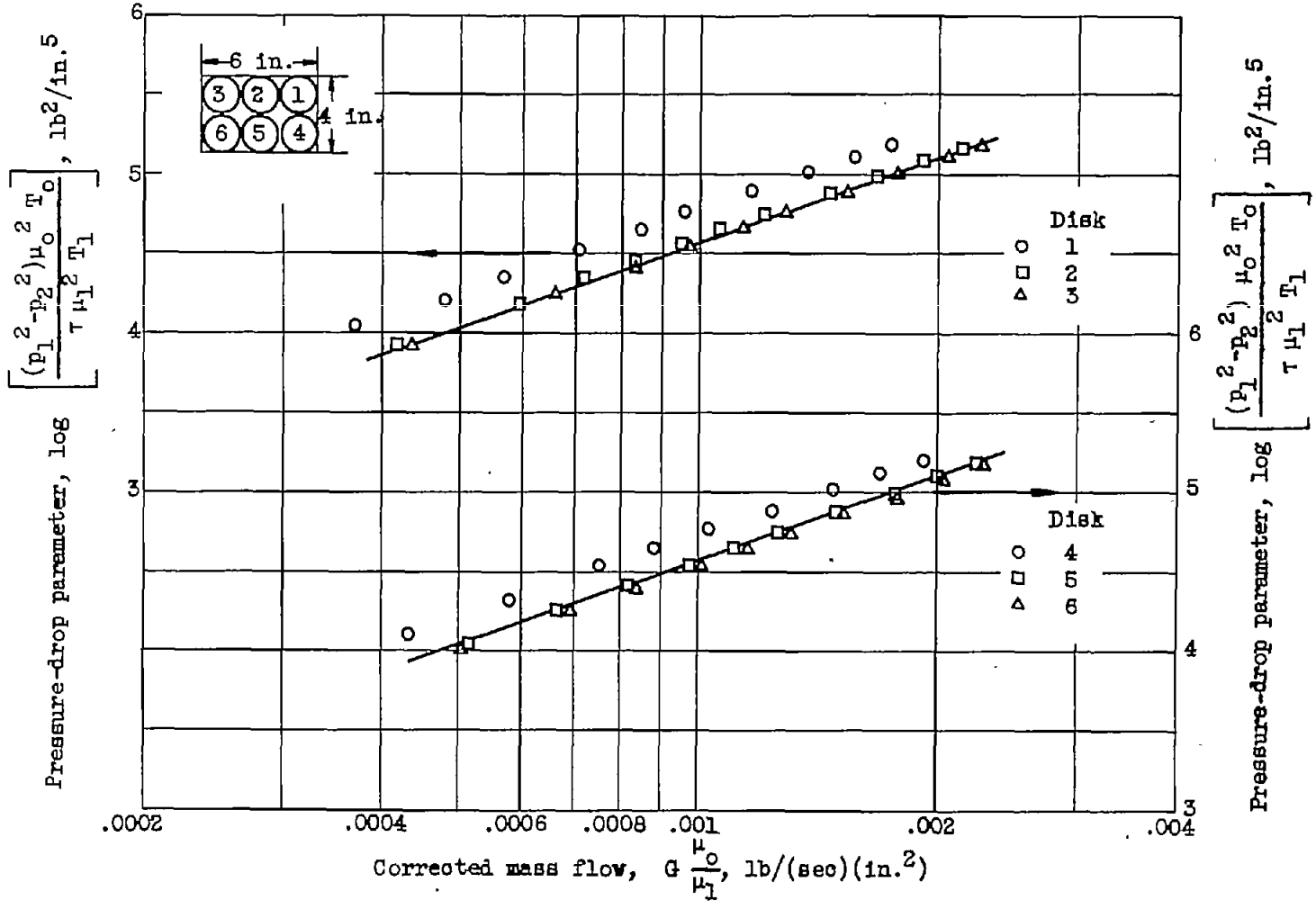

(b) Thickness reduction, 40 percent.

Figure 4. - Concluded. Uniformity of air flow through brazed 20×250 mesh wire cloth.

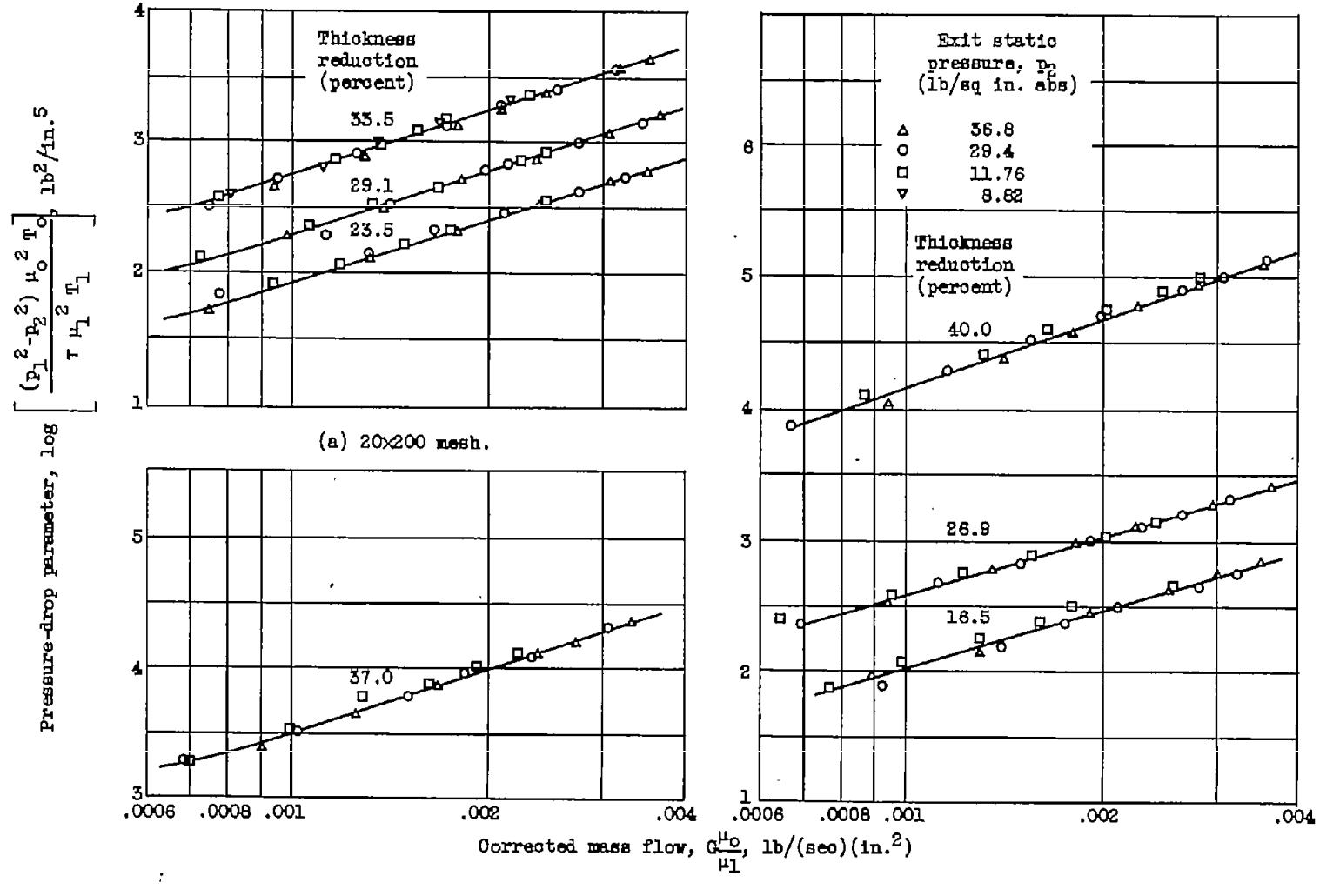

(a) 20x200 mesh.

(b) 20x250 mesh.

(c) 28x500 mesh.

Figure 5. - Correlation of air-flow data reduced to standard temperature with different pressure levels for brazed and calendered stainless-steel wire cloth.

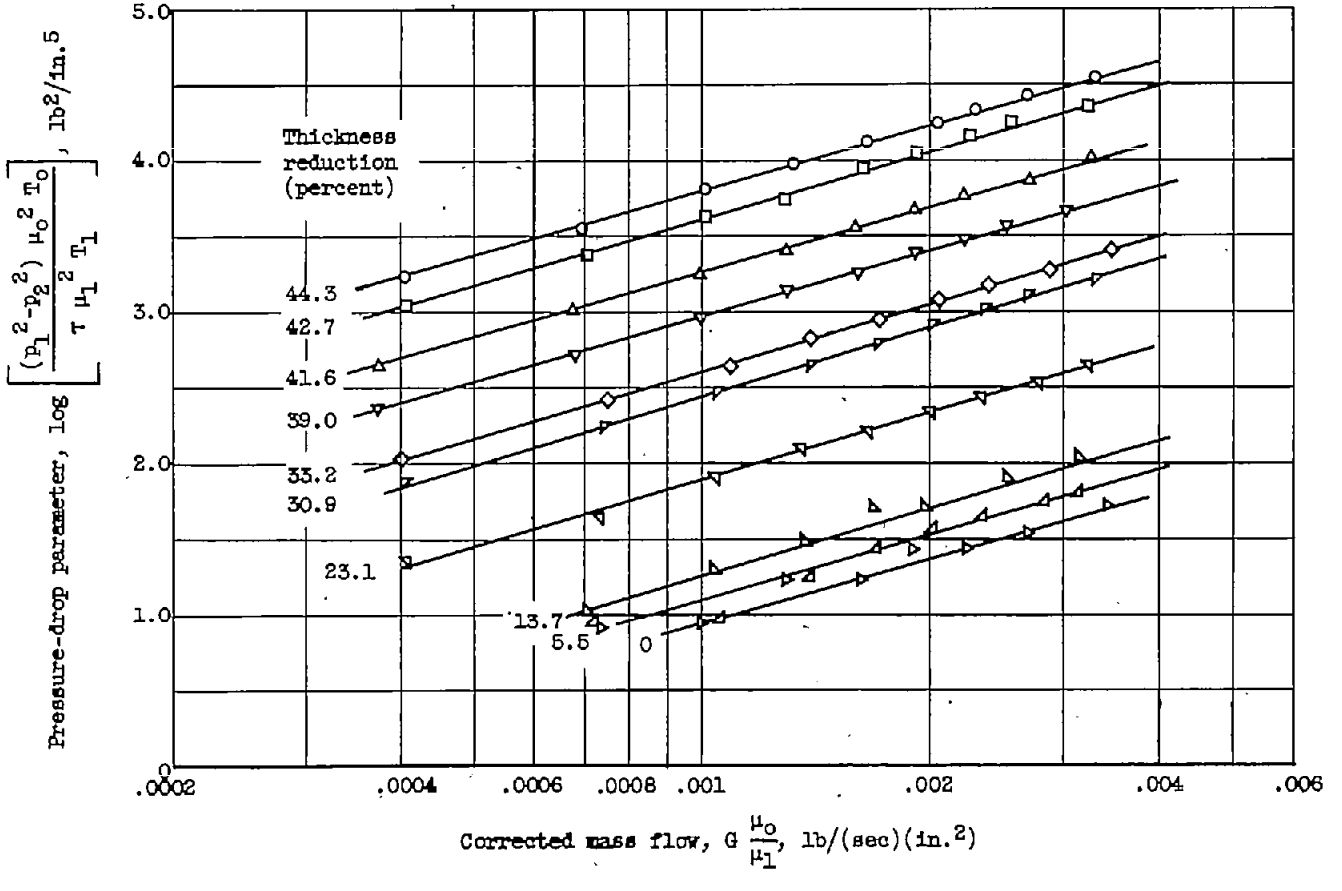

(a) Unbrazed.

Figure 6. - Correlation of air-flow data reduced to standard temperature for calendered 20X200 mesh stainless-steel wire cloth.

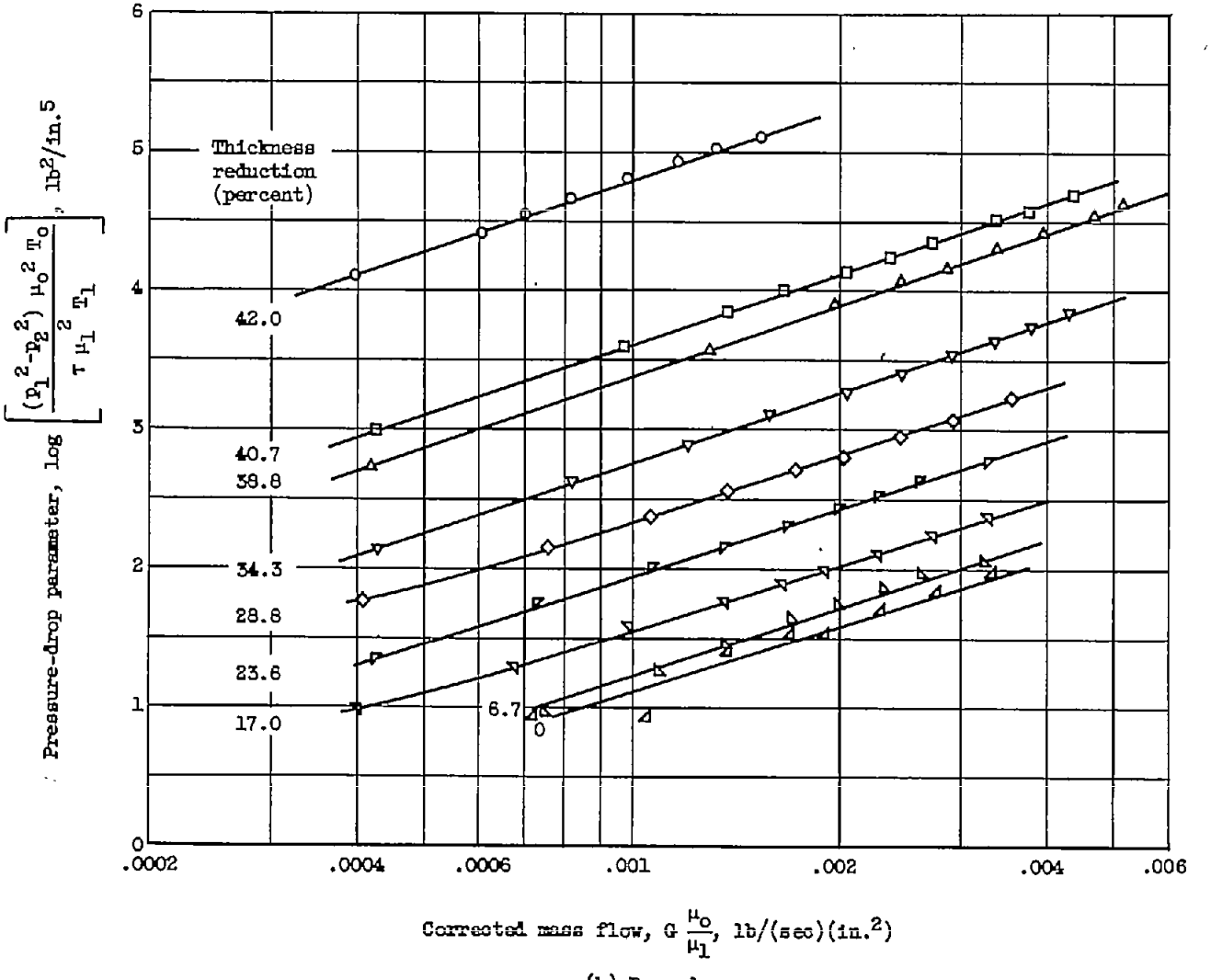

(b) Brazed.

Figure 6. - Concluded. Correlation of air-flow data reduced to standard temperature for calendered 20x200 mesh stainless-steel wire cloth.

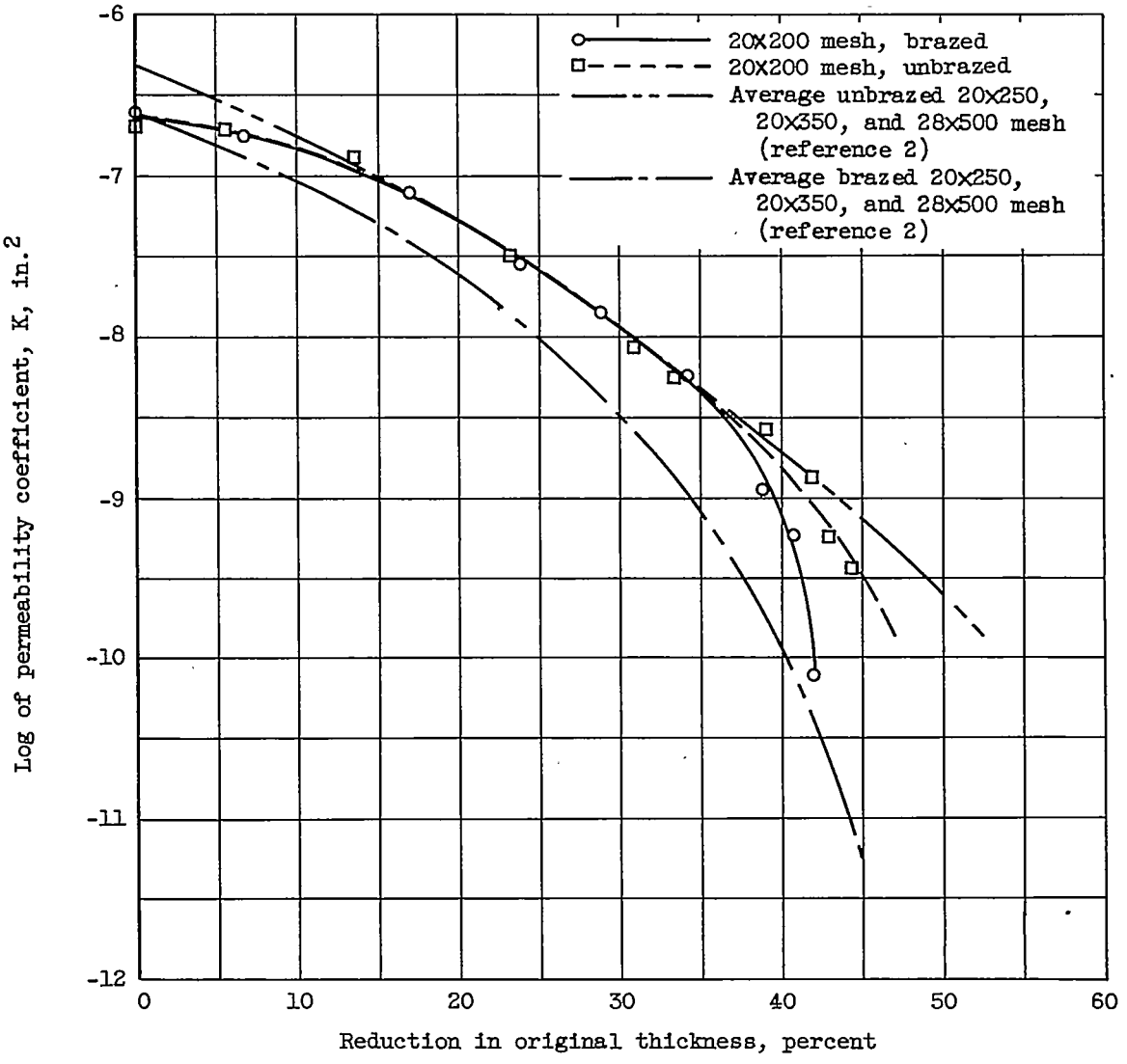

Figure 7. - Effect of calendering on permeability coefficient of brazed and unbrazed wire cloth.

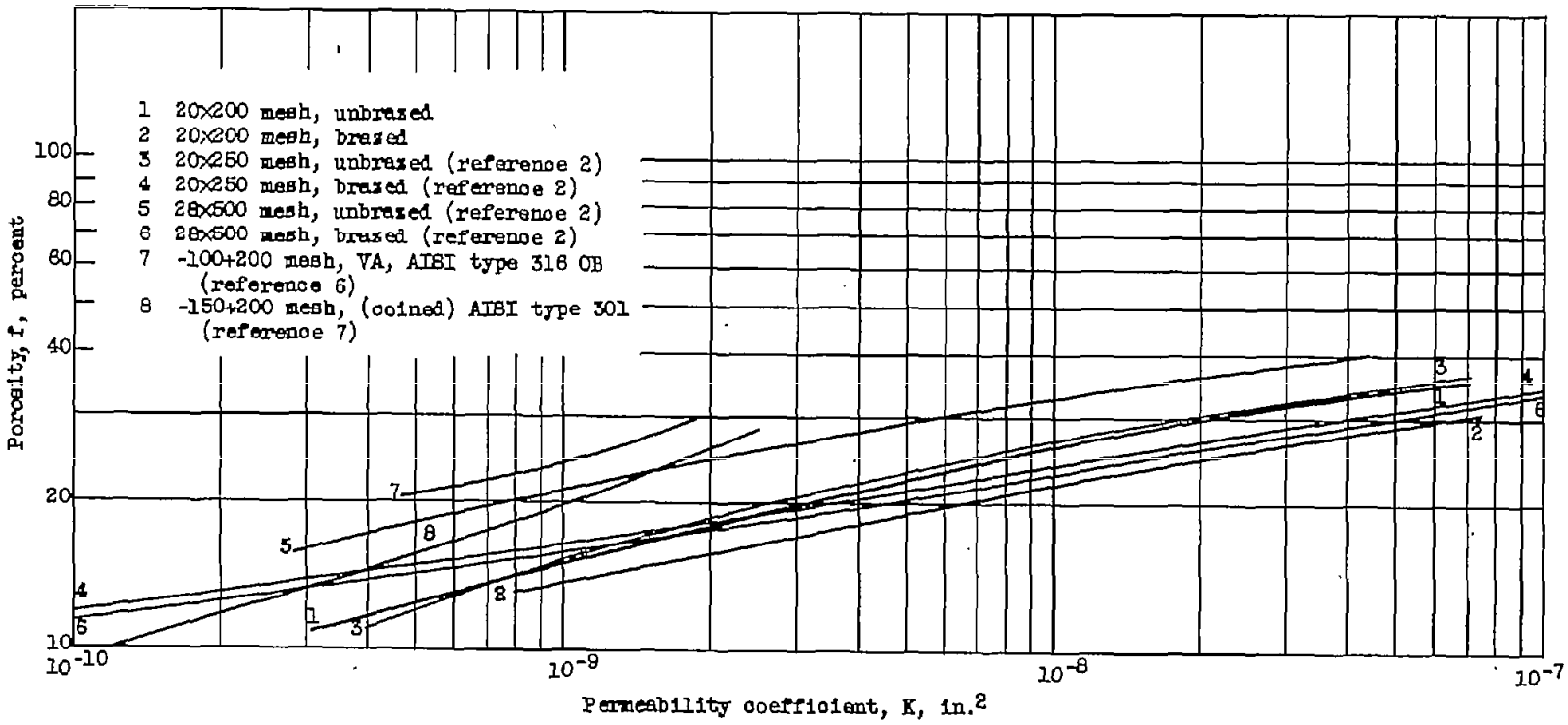

Figure 8. - Comparison of porosity and permeability coefficient for brazed and unbrazed stainless-steel wire cloth and porous sintered materials.

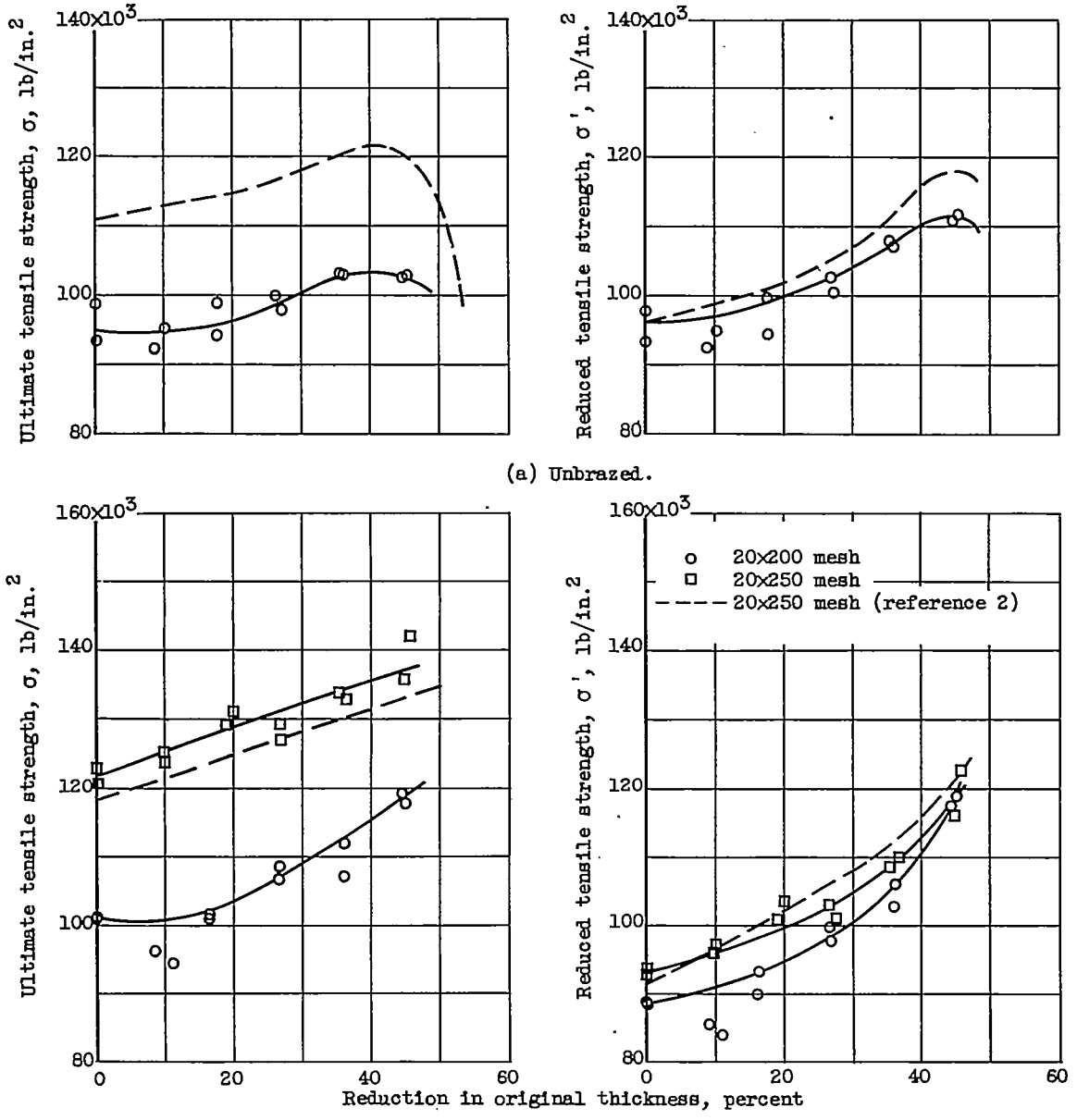

Figure 9. - Effect of calendering on tensile strength of stainless-steel 20X250 mesh unbrazed wire cloth.

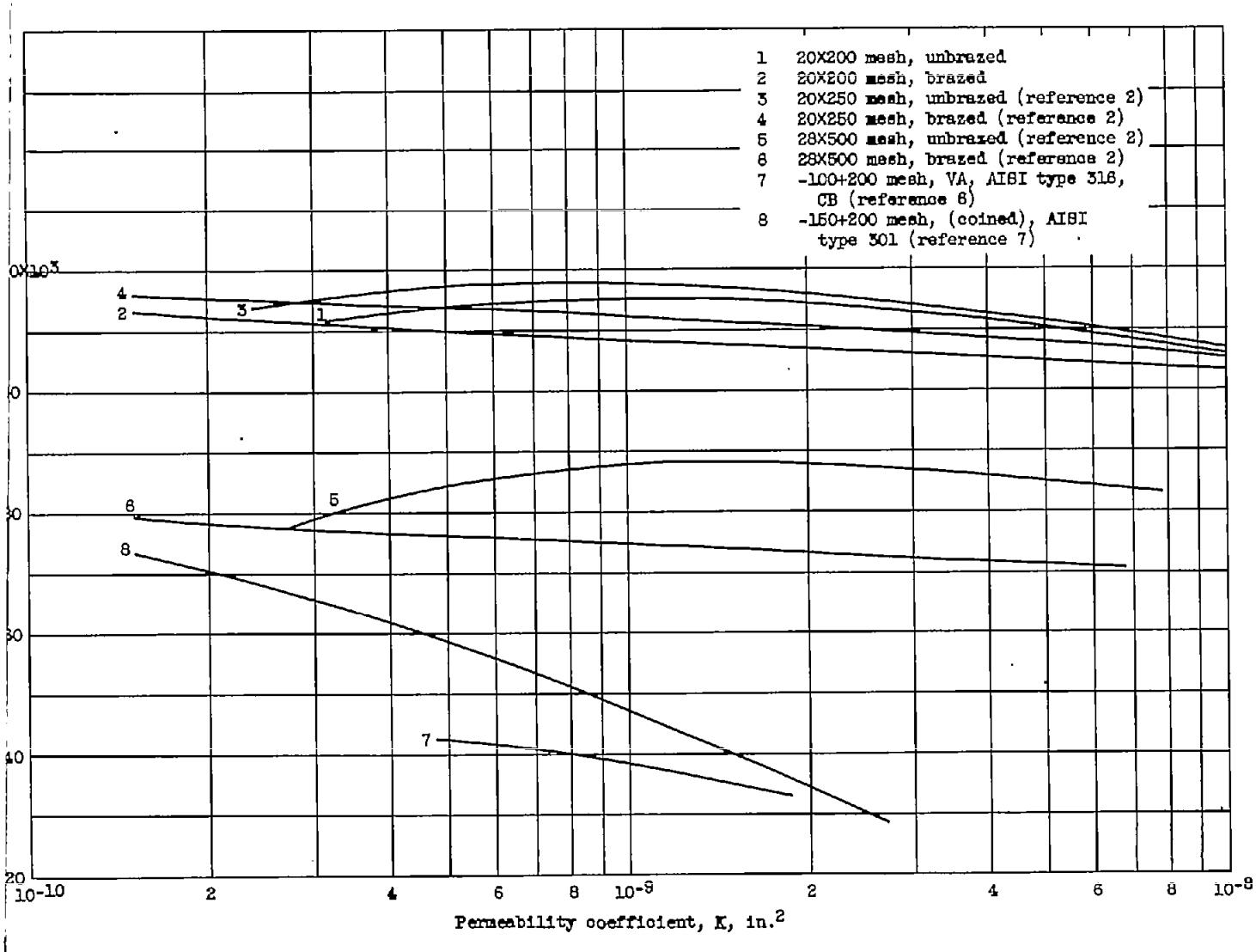

Figure 10. - Comparison of reduced tensile strength and permeability coefficient for brazed and unbrazed calendered stainless-steel corduroy wire cloth and porous sintered materials.